



**HAL**  
open science

# COORDINATION GEOMETRY OF TRANSITION METAL IONS IN DILUTE SOLUTIONS BY XANES

J. Garcia, A. Bianconi, M. Benfatto, C. Natoli

► **To cite this version:**

J. Garcia, A. Bianconi, M. Benfatto, C. Natoli. COORDINATION GEOMETRY OF TRANSITION METAL IONS IN DILUTE SOLUTIONS BY XANES. *Journal de Physique Colloques*, 1986, 47 (C8), pp.C8-49-C8-54. 10.1051/jphyscol:1986807 . jpa-00225991

**HAL Id: jpa-00225991**

**<https://hal.science/jpa-00225991>**

Submitted on 4 Feb 2008

**HAL** is a multi-disciplinary open access archive for the deposit and dissemination of scientific research documents, whether they are published or not. The documents may come from teaching and research institutions in France or abroad, or from public or private research centers.

L'archive ouverte pluridisciplinaire **HAL**, est destinée au dépôt et à la diffusion de documents scientifiques de niveau recherche, publiés ou non, émanant des établissements d'enseignement et de recherche français ou étrangers, des laboratoires publics ou privés.

**COORDINATION GEOMETRY OF TRANSITION METAL IONS IN DILUTE SOLUTIONS BY XANES**J. GARCIA<sup>(1)</sup>, A. BIANCONI\*, M. BENFATTO and C.R. NATOLI*INFN, Laboratori Nazionali di Frascati, I-00044 Frascati, Italy**\*Dipartimento di Fisica, Università "La Sapienza", I-00185 Roma, Italy*

**ABSTRACT:** The coordination geometry of transition metal ions  $\text{Cr}^{3+}$ ,  $\text{Mn}^{2+}$ ,  $\text{Fe}^{2+}$ ,  $\text{Fe}^{3+}$ ,  $\text{Ni}^{2+}$  and  $\text{Cu}^{2+}$  in aqueous solution has been studied by x-ray absorption near edge structure spectroscopy. The spectra have been analyzed in terms of successive orders of multiple scattering contributions. The effect of the absorbing central atom, oxydation state, interatomic distance of the various metal ions and the particular site structure of  $\text{Cu}^{2+}$  are discussed.

**1. INTRODUCTION**

The coordination of transition metal ions in solution has been studied by several methods which probe the pair correlation function.<sup>(1-5)</sup> However, direct information on the site geometry can only be obtained by the determination of higher orders correlation functions. It has been recently demonstrated that x-ray absorption near edge structure (XANES) spectroscopy is a direct probe of these latter<sup>(6,7)</sup> and the three atom correlation function has been extracted experimentally for the  $[\text{CrO}_4]^{2-}$  and  $[\text{MnO}_4]^-$  ions in solution.<sup>(8)</sup>

We report here the metal ion K-edge spectra of  $\text{Cr}^{3+}$ ,  $\text{Mn}^{2+}$ ,  $\text{Fe}^{3+}$ ,  $\text{Ni}^{2+}$  and  $\text{Cu}^{2+}$  ions in solution with high signal to noise ratio using synchrotron radiation. The data analysis of the XANES spectra for these ions is simplified by the structural disorder of further shells of neighbours which reduces the size of the effective absorbing cluster to the metal ion and the first coordination shell. The multiple scattering data analysis shows that octahedral geometry of water molecules around the central atom is present in all the ions studied. The effect of the ion valence state on the spectra is described in terms of different electronic configuration used to construct the final state potential and by the different metal-ligand interatomic distances. In the case of  $\text{Cu}^{2+}$  regular octahedral geometry was found and the tetragonal Jahn Teller distortion expected for this ion was not observed. A careful analysis of the EXAFS and XANES spectra supports the conclusion that either the static distortion is less than 0.3 Å or a dynamical Jahn Teller distortion is present in this ion.

**2. EXPERIMENTAL AND CALCULATION**

The XANES and EXAFS spectra of transition metal ions have been measured at the Frascati

<sup>(1)</sup> Permanent Address : Departamento de Termologia, Universidad de Zaragoza, Zaragoza, Spain

Synchrotron Radiation Facility, using a Si(111) channel-cut single crystal monochromator and variable entrance slits in the range 0.2-1mm. Aqueous solutions at different concentrations have been prepared and the value of pH has been controlled in order to have the hydrated species. Different mylar thick cells have been used in transmission experiments. In the data analysis the pre-edge absorption background was subtracted. The MS calculation for the octahedral and tetrahedral clusters formed by the central metal and the oxygen ligands were made using the usual X- $\alpha$  potential and Mattheis prescription. Hydrogen atoms were neglected. The approximation Z+1 and different electronic configurations to construct the central ion potential were used.

### 3. RESULTS AND DISCUSSION

#### 1. Octahedral complexes

Spectra of CrCl<sub>3</sub>, FeCl<sub>3</sub>, MnCl<sub>2</sub> and NiCl<sub>2</sub> 50mM aqueous solution are reported in figure 1 over a 120 eV energy range. These spectra characteristic of octahedral oxygen geometry (6,7), show the presence of two features near the absorption edge (labeled A and B) which are better resolved in the case of divalent ions than in the trivalent ones. In fact, the B feature in the Cr<sup>3+</sup> spectra reaches the same height as the main peak A, an intermediate situation occurs in the Fe<sup>3+</sup> spectrum whereas for divalent ions feature A is much higher than feature B. The different spectral shape for divalent and trivalent ions provides indication that changes on the shape in the XANES spectra can also be caused by the different oxidation state. Multiple scattering calculations for the 1s(A<sub>1</sub>)- $\epsilon$ p(T<sub>1u</sub>) transitions in MeO<sub>6</sub> octahedral clusters (Me= Cr, Mn, Fe, Ni) are reported in figure 2 where we use the interatomic distances given in literature (3). The shape of the calculated spectra corresponds closely to the experimental ones, showing the difference between the spectrum of divalent and trivalent metals.

In terms of multiple scattering contributions, the main line A for octahedral clusters is determined by a full multiple scattering resonance where all the multiple scattering contributions  $X_n$  to the total cross section  $\alpha$ ,  $\alpha = \alpha_0(1 + \sum_{n=2} X_n)$ , are in phase. (7) We report in figure 3 the expansion of the cross section in the different multiple scattering components for the CrO<sub>6</sub> cluster. Although higher orders of multiple scattering are not negligible above 60 eV, the destructive interference between pair of consecutive terms, i.e.  $X_3$  and  $X_4$ , is the reason why only the second order term is relevant above this energy. This seems a general physical effect for octahedral clusters in which the relevant multiple scattering events corresponds to that of collinear configuration. In the energy range between the main resonance A and 50 eV above zero the structure is mainly determined by  $X_2$  and  $X_3$ . To test the capability to determine the geometry we have performed calculations for tetrahedral clusters in figure 4. In the three upper spectra of MnO<sub>4</sub><sup>-</sup>, CrO<sub>4</sub><sup>2-</sup> and VO<sub>4</sub><sup>3-</sup> we have used the real metal ion-ligand distance, whereas for the FeO<sub>4</sub> and CuO<sub>4</sub> spectra we have taken the same distance as for the octahedral case. We notice two effects: a dependence of the shape of the spectra on the distance inside the two tetrahedral groups and an overall difference of the tetrahedral spectra from their octahedral counterpart. Also for the FeO<sub>4</sub> and CuO<sub>4</sub> theoretical spectra the total cross section is reproducible up to 100 eV with the sum of the  $X_2$  and  $X_3$  terms, which could allow the determination of the three particle correlation function in these systems. (7,8) The multiple scattering higher orders terms in MeO<sub>4</sub> tetrahedral clusters go to zero more quickly than in octahedral clusters and the take over of the EXAFS regime is not determined by a destructive interference effect.

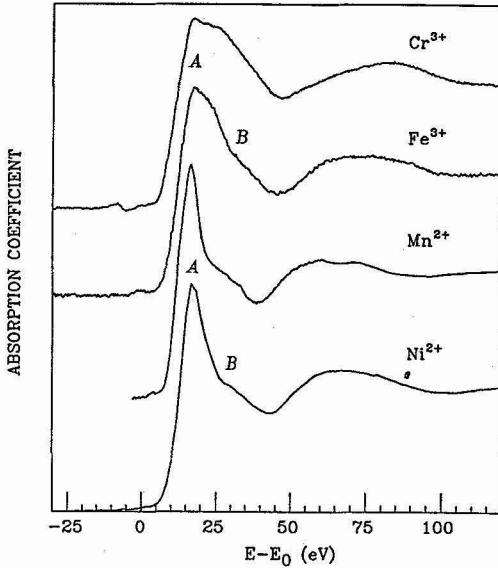


Fig 1. Experimental K-metal XANES spectra of  $\text{Cr}^{3+}$ ,  $\text{Fe}^{3+}$ ,  $\text{Ni}^{2+}$  and  $\text{Mn}^{2+}$  ions in 50 mM aqueous solution of their chlorides. The zero of the energy scale is fixed at the first prepeak structure.

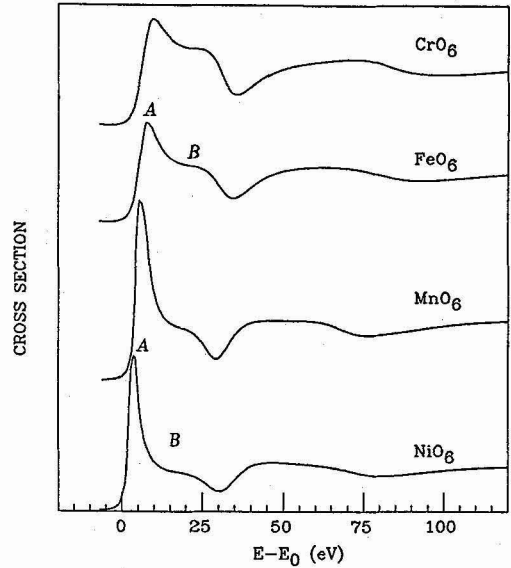


Fig 2. Theoretical XANES spectra for  $\text{CrO}_6$ ,  $\text{FeO}_6$ ,  $\text{MnO}_6$  and  $\text{NiO}_6$  octahedral clusters. The interatomic distances used are:  $d(\text{Cr-O})=2.0$  Å,  $d(\text{Fe-O})=2.02$  Å,  $d(\text{Mn-O})=2.17$  Å and  $d(\text{Ni-O})=2.06$  Å.

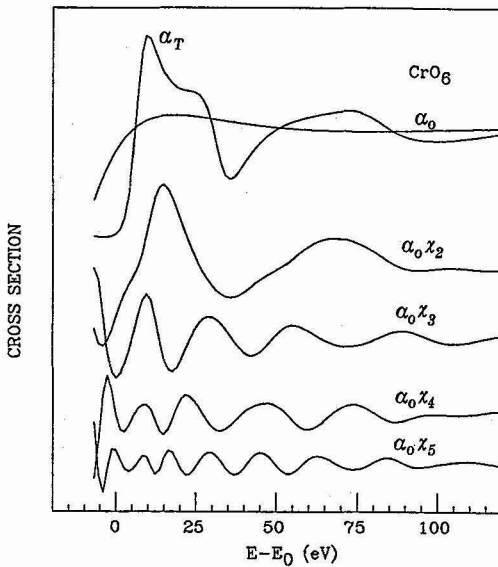


Fig 3. Theoretical total cross section  $\alpha$  and its multiple scattering contributions  $\alpha_0$ ,  $\alpha_0\chi_2$ ,  $\alpha_0\chi_3$ ,  $\alpha_0\chi_4$  and  $\alpha_0\chi_5$  for the  $\text{CrO}_6$  cluster.

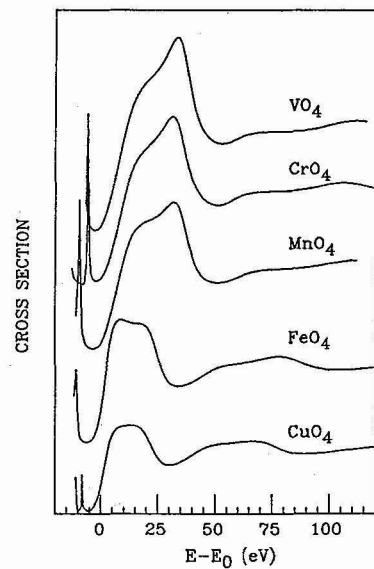


Fig 4. Theoretical full multiple scattering calculations of XANES spectra for tetrahedral clusters.

## 2. Study of valence and distance dependence in $\text{Fe}^{2+}/\text{Fe}^{3+}$ system.

The effect of the valence state is studied for the  $\text{Fe}^{2+}$ - $\text{Fe}^{3+}$  system by comparing the experimental  $\text{Fe}^{3+}$  spectrum with that of  $\text{Fe}^{2+}$  measured in dispersive mode by Fontaine et al.<sup>(9)</sup> In the lower panel of figure 5 we report these spectra plotted in an absolute energy scale obtained by calibration with the spectra of iron metal. The calculated spectra for  $\text{FeO}_6$  cluster with interatomic distances 2.10 Å ( $\text{Fe}^{2+}$ -O distance) and 2.02 Å ( $\text{Fe}^{3+}$ -O distance)<sup>(3,10)</sup> are plotted in the upper panel of this figure. The  $\text{Fe}^{2+}$  spectrum exhibits the same shape as the other spectra of divalent metals. In order to study the effect of changes of distances and/or oxidation state, we have performed for the  $\text{Fe}^{3+}$  octahedron two different calculations; in the first, we have used the same excited potential inside the Fe muffin-tin sphere as that used for the calculation of  $\text{Fe}^{2+}$  octahedron, and in the second, we have changed the starting electronic configuration used to construct the potential in the excited state. In the first case we do not find any change of the relative height of the A and B structures, only a little shift of the inflexion point of the rising edge and a larger separation of the structures, in such a way that by rescaling the spectra we can superpose them. In the second case, we find a change of the relative height of the A and B structures and a large energy shift.

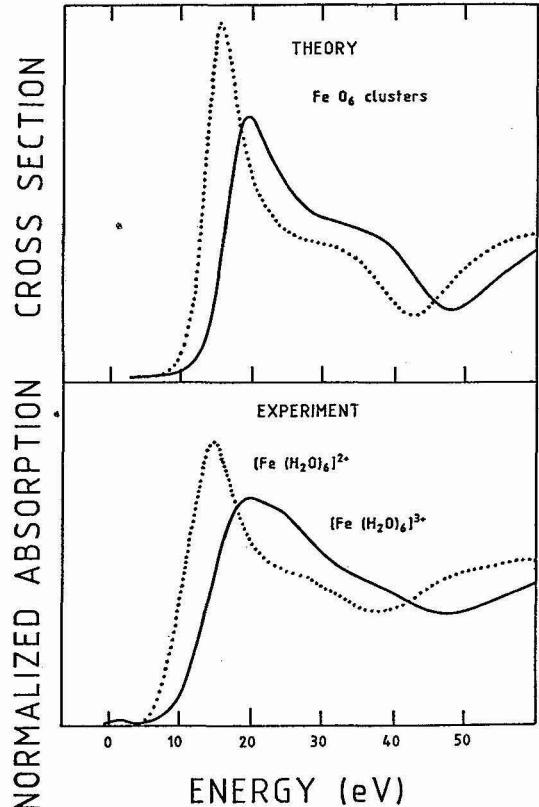


Fig 5. Experimental Fe K-edge spectra of  $\text{Fe}^{2+}$  and  $\text{Fe}^{3+}$  ions in water solutions (lower panel) and theoretical calculations of octahedral  $\text{FeO}_6$  clusters (upper panel).

This last calculation which is plotted in the upper panel of fig. 5 together the  $\text{Fe}^{2+}$  theoretical spectrum in the same absolute scale reproduce well the experimental situation. From this analysis, we can say that the chemical energy shift is determined by the cooperation of different factors like the interatomic distance, the electronic state of the absorbing atom and to the XPS chemical shift due to the initial state.<sup>(11)</sup> The other important fact, that we want to emphasize, is the effect of the oxidation state on the shape of the spectrum in the first 30 eV above the rising edge, for which a detailed description requires a good knowledge of the central atomic potential. The comparison between the different multiple scattering contributions for the  $\text{Fe}^{2+}$  and  $\text{Fe}^{3+}$  shows that this different behaviour is connected with small changes in the central atom phase shifts in the region near the edge.

### 3. The Jahn Teller distortion around the $\text{Cu}^{2+}$ site in solution

The XANES spectrum of  $\text{Cu}^{2+}$  ion at 50 mM concentration is reported in figure 6. The spectrum is similar to the spectra of octahedral sites but the intensity of peaks A and B are weaker than in the other cases. The multiple scattering calculation for a undistorted octahedral coordination is reported in fig 6. The comparison shows that there is a significant difference in the ratio of features the A and B. We have considered this point as an indication of a distortion of the

octahedral site. A calculation for a tetragonally distorted octahedron with Cu-O distances on the basal plane of 2. Å and with two axial ligands at 2.6 Å is reported. The calculated spectrum predicts the presence of two clear structures on the low ( $T_1$ ) and high ( $T_2$ ) energy sides of the main line A. Also the calculation for an octahedron with two axial chlorine (Cl) at 2.6 Å atoms is reported and exhibits similar  $T_1$  and  $T_2$  features. We have also supposed a possible square plane coordination and the relative calculated spectrum for the  $\text{CuO}_4$  cluster is reported. This spectrum is characterized by a broad feature  $T_1$  on the rising edge and by a weaker main line A because of the reduced number of neighbouring atoms. The validity of this calculation is confirmed by comparison with the spectrum of stoichiometric CuO solid sample where the square plane coordination is well established. By comparing the experimental spectrum for

$\text{Cu}^{2+}$  in solution we find that it does not show any detectable structure on the rising edge of the main line A. By performing calculations for clusters with increasing axial distortion we have found that the feature  $T_1$  moves with the axial distance. For an elongation of the axial distance  $\Delta d$  smaller than 0.3 Å the shoulder  $T_1$  can not be resolved. Therefore we estimate that the Jahn-Teller axial distortion is smaller than 0.3 Å. This result is confirmed by a careful EXAFS data analysis using curved waves which indicates an asymmetry in the radial distribution function not larger than 0.3 Å. These results support the conclusion that the Jahn Teller effect in  $\text{Cu}^{2+}$  ion in solution do not produce a large (0.6 Å) static tetragonal distortion but the distortion has to be considered of the dynamical Jahn-Teller type. Recent experiments of XRD on  $\text{Cu}^{2+}$  solutions are in agreement with the precedent conclusions in that this distortion presents large Debye Waller factors.<sup>(12-13)</sup>

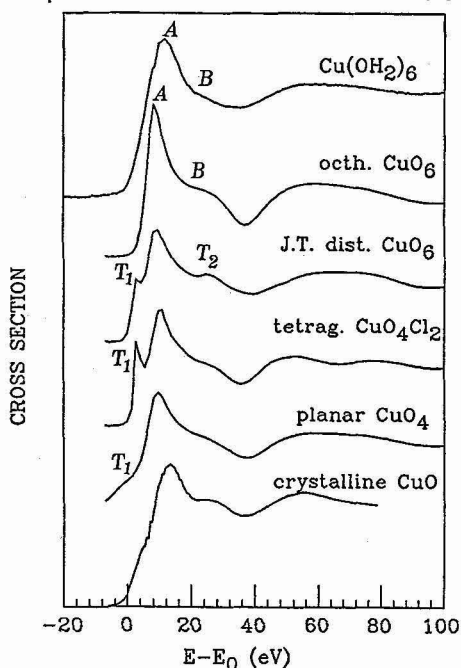


Fig 6. The experimental spectrum of  $\text{Cu}^{2+}$  in solution is compared with the crystalline CuO spectrum and with theoretical calculations for different Cu coordination geometries.

#### REFERENCES

1. P.V. Giaquinta, M.P. Tosi and N.H. March, Phys. Chem. Liq. **13**,1(1983)
2. D.R. Sandstrom, Nuovo Cimento **3D**,825,(1984)

3. G. Licheri and G. Pinna in "EXAFS and Near Edge Structure" Springer Series in Chemical Physics vol. 27, 240 (1983)
4. P. Lagarde, A. Fontaine, D. Raoux, A. Sadoc and P. Migliardo, J. Chem. Phys. 72, 3061 (1980)
5. J.E. Enderby and G.W. Neilson, Rep. Prog. Phys. 44, 593 (1981)
6. A. Bianconi, J. Garcia, A. Marcelli, M. Benfatto, C.R. Natoli and I. Davoli, J. de Physique, 46, C9-101, (1985)
7. M. Benfatto, C.R. Natoli, A. Bianconi, J. Garcia, A. Marcelli, M. Fanfoni and I. Davoli, Phys. Rev. B., in press.
8. J. Garcia, M. Benfatto, C.R. Natoli, A. Bianconi, I. Davoli, A. Marcelli. Solid State Comm. 58, 595 (1986)
9. Fontaine et al. to be published
10. R. Camini and M. Magini, Chem. Phys. Lett. 61, 40, (1979)
11. C.R. Natoli in "EXAFS and Near Edge Structure III" Springer Proc. in Physics 2, 43 (1984).
12. G. Licheri, A. Musinu, G. Paschina, G. Piccaluga, G. Pinna and A.F. Sedda, J. Chem. Phys. 80, 5308 (1984).
13. A. Musinu, G. Paschina, G. Piccaluga and M. Magini, Inor. Chem. 22, 1184, (1983)